Topological Semimetals and Insulators for Low-Temperature Thermoelectric Cooling

Yu Pan[#], Bin He[##], Dong Chen, Haihua Hu, Walter Schnelle and Claudia Felser

Topological semimetals and insulators are crucial to the field of thermoelectrics, particularly for low-temperature cooling. Our studies focus on the thermoelectric transport properties of single-crystal topological materials and the relationships between topological properties and thermoelectric applications. In systems with broken time-reversal symmetry, such as magnetic Weyl semimetal $YbMnBi_2$, a giant anomalous Nernst thermopower is observed, along with a large thermoelectric Hall conductivity. Similar anomalous signals have been observed in the Dirac system CsV_3Sb_5, which exhibits chiral charge density waves. In multiband topological semimetals, a large ordinary Nernst signal can be anticipated, as is observed in WTe_2 and $TaAs_2$. Finally, in topological insulator $Bi_{88}Sb_{12}$, which exhibits linear band dispersion, a strong magneto-Seebeck effect has been recorded. This system has shown a dimensionless figure of merit zT of 1.7, which is 50% higher than previously highest zT, making it particularly promising for low-temperature thermoelectric cooling.

Thermoelectric materials can directly convert heat into electricity and vice versa. The conversion efficiency is directly related to the dimensionless figure of merit, zT. The electronic band structure plays a pivotal role in contemporary thermoelectric research. In addition to materials with intrinsically low thermal conductivity, materials with high Seebeck/Nernst coefficients and low resistivities are favorable for high-performance thermoelectric applications, particularly thermoelectric cooling. Topological materials, with their distinctive band structures, are promising candidates for thermoelectric materials with desirable properties.

The relationship between topology and thermoelectrics can be traced back to the discovery that good thermoelectric materials are also topological insulators. It is widely recognized that, while the band topology has limited impact on the zero-field Seebeck coefficient, topological semimetals typically exhibit a pronounced transverse thermoelectric response, commonly referred to as the Nernst signal. Furthermore, in the presence of an external magnetic field, a strong magnetic response in the Seebeck coefficient can be anticipated owing to the nature of the topological band structure.

In topological semimetals, linear band crossings with fourfold degeneracy generate Dirac semimetals. Theoretically, when the time-reversal symmetry (TRS) is broken, Weyl points are created and a large anomalous Nernst effect (ANE) can be anticipated. Furthermore, because of the high mobility of electrons and holes in topological semimetals, a large ordinary Nernst effect (ONE) can be expected. The strong compensation between electrons and holes causes the ONE to be orders of magnitude higher than that of classic metals. Finally, a large non-saturating magneto-Seebeck effect can be anticipated when the energy band has a linear band dispersion relation. We have experimentally proven these ideas and, more importantly, achieved a large ANE, giant ONE, strong magneto-Seebeck effect, and high magneto zT in topological materials.

Anomalous Nernst Effect in Unconventional Topological Semimetals

The ANE is mostly observed in materials with broken TRS, which, in practice, refers to ferromagnets. A large Berry curvature is generated with the broken TRS; consequently, large ANE signals are often observed. However, ferromagnets usually have low electron mobility because of heavy *d* band and strong magnetic scattering. This is unfavorable for high-performance transverse thermoelectric materials because achieving a large zT requires both high thermopower and low resistivity. Counterintuitively, we discovered a strong ANE response in canted antiferromagnets. Because of the *p–d* hybridization and antiferromagnetic nature of these materials, the electrons have a small effective mass and minimal magnetic scattering effect; therefore, high mobility can be maintained, accompanied by a large transverse power factor. Moreover, the ANE is also observed in CsV_3Sb_5, a Dirac semimetal with a chiral charge density wave that equivalently breaks the TRS.

$YbMnBi_2$ has been confirmed to be a magnetic Weyl semimetal owing to its canted magnetic structure. The Weyl points were identified by angle-resolved photoemission spectroscopy, as shown in Figure 1a, while giant ANEs were observed when a temperature gradient and magnetic field are applied across the *bc* and

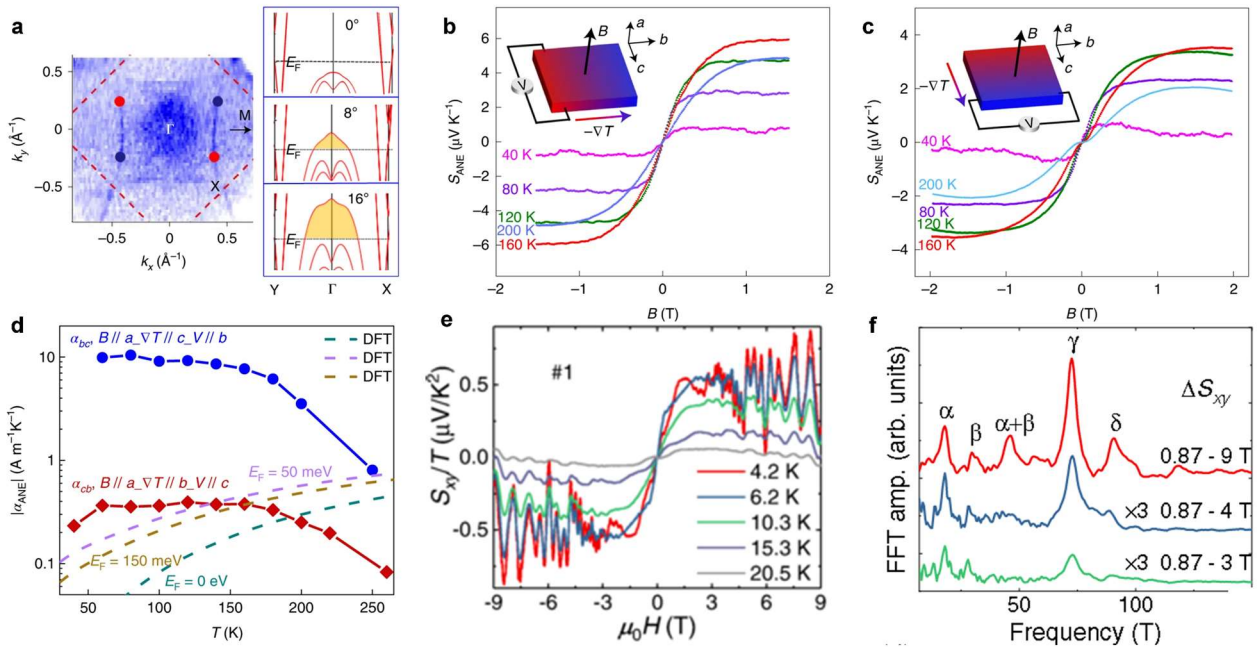

Fig. 1: (a) Weyl points and band simulation in $YbMnBi_2$. (b) and (c) ANE of $YbMnBi_2$ along different crystals directions. (d) Experimental and theoretical temperature dependent thermoelectrical Hall conductivity. (e) ANE of CsV_3Sb_5 at different temperature. (f) Frequencies of different pockets in CsV_3Sb_5.

ab planes, respectively. Figures 1b and 1c show the ANE measurements along different directions. The largest ANE values were 6 and 3 μV K^{-1}, respectively, and the largest anomalous Nernst conductivity was 10 A K^{-1} m^{-1}, which is much higher than that of conventional ferromagnets, as shown in Figure 1d. The electronic structure and transport properties were calculated by density functional theory (DFT) at different canting angles. Interestingly, the experimental thermoelectric Hall conductivity has a negative temperature dependence and is much higher than the DFT-calculated results. This discrepancy was concluded to be caused by a combination of intrinsic and extrinsic contributions. Moreover, it indicates that a large extrinsic ANE – much stronger than the contribution of Berry curvature – is anticipated in the presence of broken TRS, high mobility, and strong spin–orbit coupling.

In addition to well-established magnetic Weyl semimetals, the ANE is also observed in the unconventional Dirac semimetal CsV_3Sb_5. CsV_3Sb_5 has a V-based kagome lattice with rich physical phenomena, including Dirac cones, van Hove singularities, and flat bands. The Fermi energy of CsV_3Sb_5 is close to the Dirac points; therefore, it generally exhibits the behavior of a Dirac semimetal with high carrier mobility. Moreover, a charge density wave transition is observed near 90 K, below which the Fermi surface is nested and a chiral charge order appears. This chiral charge order breaks the TRS and gives rise to anomalous transport behaviors. High-quality CsV_3Sb_5 crystals exhibit a residual resistance ratio of over 300 and a superconducting transition at approximately 4 K. We observed a strong ANE below 30 K, reaching a maximum of approximately 3 μV K^{-1}, as shown in Figure 1e. Strong quantum oscillation was detected during the ANE measurement, from which five frequencies were obtained. Compared with the electrical transport results, we discovered a previously unreported peak from thermoelectric transport, as illustrated in Figure 1f.

Large Ordinary Nernst Effect in Topological Semimetals

In addition to the large ANE of magnetic Weyl semimetals, a large ONE is also anticipated in topological semimetals, wherein the electrons and holes are both highly mobile and nearly compensated. The ONE is usually negligible in classic metals owing to Sondheimer cancelation. However, the ONE in multicarrier systems is a product of the Seebeck coefficient and mobility. Because topological semimetals usually contain high-mobility carriers, their ONE can be orders of magnitude higher than that of classical metals. In this section, we focus on the ONE in a transition-metal dichalcogenide, WTe_2, and a transition-metal dipnictide, $TaAs_2$.

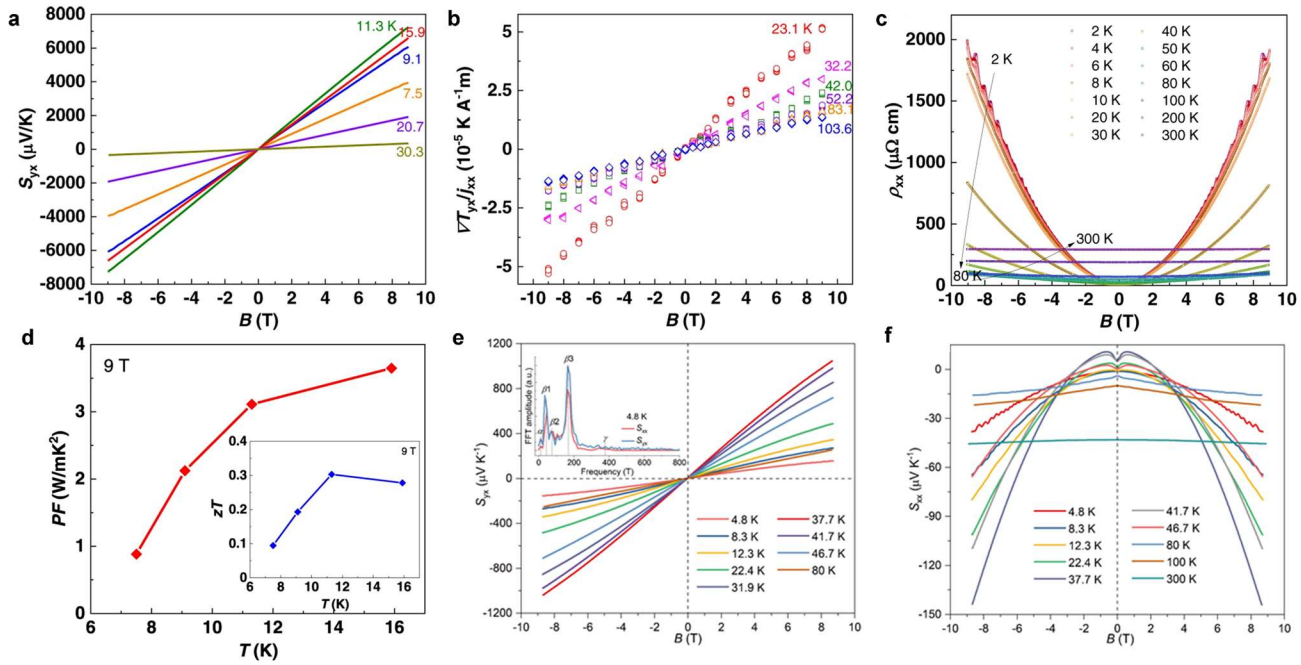

Fig. 2: (a) Large Nernst signal and optical image of WTe_2 crystal. (b) Ettingshausen coefficient and (c) giant magnetoresistance of WTe_2. (d) Temperature-dependent power factor (PF) of WTe_2. (e) Large Nernst thermopower and (f) magneto-Seebeck coefficient of $TaAs_2$.

WTe_2 is a type-II Weyl semimetal with nearly perfect electron–hole compensation; consequently, it exhibits colossal magnetoresistance (MR). Furthermore, because of this compensation, a giant ONE is expected in WTe_2. We discovered that WTe_2 has good flexibility, which fits the idea of flexible thermoelectric materials, as shown in Figure 2a. Using thermoelectric measurements, we observed a linear, non-saturating ONE signal below 30 K, as shown in Figure 2a, with a maximum of over 7 mV K^{-1} at 11 K. Figure 2b shows a pronounced Ettingshausen coefficient, which is strongly related to the ONE signal. The colossal MR was repeated, as shown in Figure 2c. The Nernst power factor was calculated to be over 3 W K^{-1} m^{-2} at 16 K – second only to that of elemental Bi – making it a promising low-temperature thermoelectric cooling material, as shown in Figure 2d.

$TaAs_2$ is another candidate topological semimetal for a large ONE. In addition to electron–hole pairs, it has an additional massive Dirac pocket at the Fermi energy. Consequently, the electron-hole compensation is not so ideal as that for WTe_2. The largest ONE signal for $TaAs_2$, as shown in Figure 2e, is approximately 1 mV K^{-1} at 40 K. Furthermore, owing to its imperfect compensation, a large magneto-Seebeck effect is observed, as shown in Figure 2f. The cause for this large magneto-Seebeck is from the massive Dirac band.

Magneto-Seebeck Effect in Topological Materials

Heavily doped high-performance thermoelectric semiconductors are commonly modeled by the single parabolic band model, in which the energy-momentum relation is parabolic and no magneto-Seebeck is anticipated. Experimentally, a small magneto-Seebeck effect is often observed because of the energy-dependent scattering time. However, topological materials usually have linear bands, which, in theory, are capable of generating strong magneto-Seebeck signals. $TaAs_2$ is a prominent example of such materials owing to its massive Dirac band and non-saturating magneto-Seebeck response. However, the $TaAs_2$ system requires a high thermal conductivity and high field to achieve this. Therefore, it is preferable to search for a low-field material with high thermoelectric performance.

We focused on the first established topological insulator, Bi–Sb. Elemental Bi is a classic semimetal with Dirac electrons in its conduction bands. By alloying with over 7 molar percent of Sb, it can be converted into a topological insulator. We investigated $Bi_{88}Sb_{12}$ because this composition has a large band gap. The crystal structure and the high-quality crystal image are shown in Figure 3a. Mirror-like shiny crystals were grown using a zone-melting method. The temperature dependence of the magneto-Seebeck coefficient is presented in Figure 3b. Unlike metals, which have a

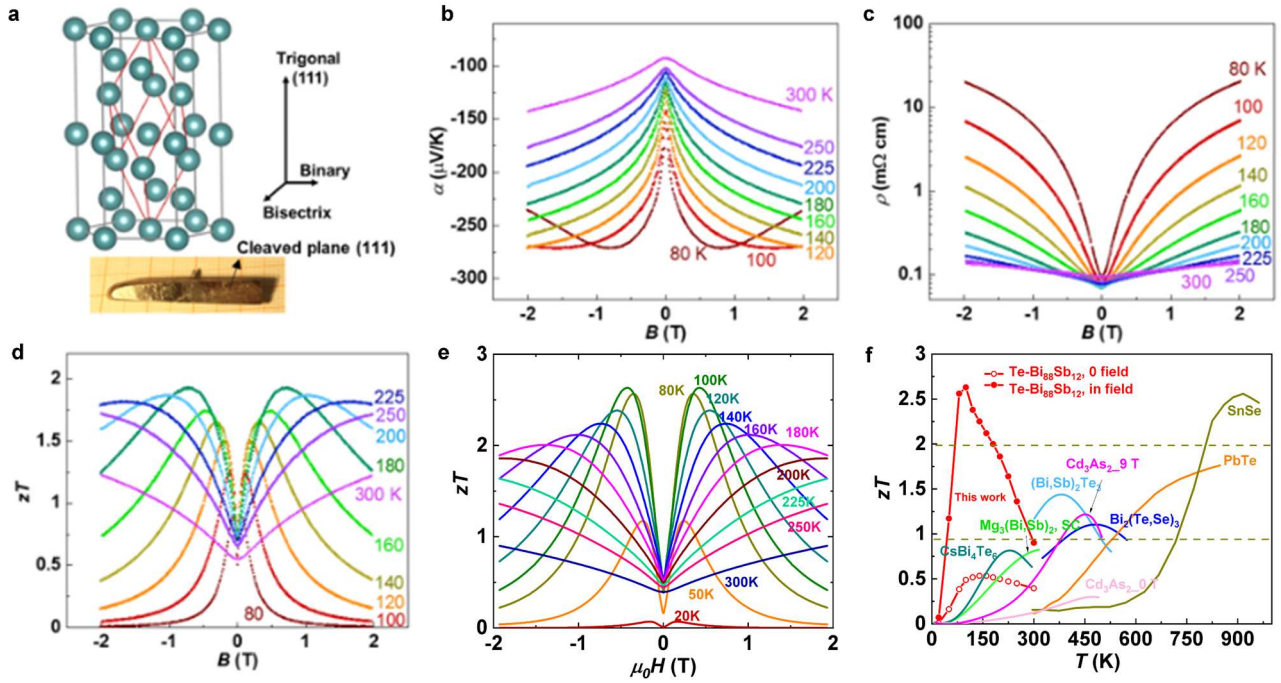

Fig. 3: Crystal structure and optical image of $Bi_{0.88}Sb_{0.12}$ single crystals. (b) Field dependent Seebeck coefficient of Bi-Sb alloy at different temperature. A nearly saturation behavior is observed around 2 T. (c) Field dependent resistivity at different temperature. A large field response is observed due to two-carrier effect. (d) Field dependent figure of merit zT of Bi-Sb alloy. (e) zT of Te doped $Bi_{88}Sb_{12}$ alloy. (f) Comparison of the high performance Bi-Sb alloy with other thermoelectric materials.

marginal field response, $Bi_{88}Sb_{12}$ exhibited a Seebeck coefficient that was almost twice the zero-field value at low temperatures. A large MR was observed as well, as shown in Figure 3c. Furthermore, the figure of merit *zT* is shown Figure 3d. With the large magneto-Seebeck coefficient, the in-field *zT* is much higher than the zero field results, reaching nearly 2 at 180 K. For the undoped $Bi_{88}Sb_{12}$ alloy, it stands as a favorable platform for further optimization. Hence, we doped 10 ppm Te into the mother alloy of the $Bi_{88}Sb_{12}$. The in-field *zT* after doping, is shown Figure 3e. Subsequent doping, the low temperature *zT* is over 2.5 at 100 K, making it a promising thermoelectric cooling material at liquid nitrogen temperature.

Compared to other high-performance thermoelectric materials, as shown in Figure 3f, the *zT* of our Bi-Sb alloy is comparable to the best high temperature material SnSe and PbTe. Moreover, our materials is also comparable to the best room temperature cooling material Bi_2Te_3. This wide range high performance allows us to build a multi-stage cooling device that functions from room temperature all the way to 100 K.

Outlook

A primary direction for future research is to investigate the thermoelectric transport in kagome materials. For instance, the in-plane thermoelectric transport of CsV_3Sb_5 has been well-understood, it will be of interest to investigate its out-of-plane thermoelectric transport and utilize it as a transverse thermoelectric material. In addition to the V based system, a series of kagome lattices formed by magnetic elements (Mn, Co, and Ni) have been predicted to exhibit exotic transport properties. Compounds like RMn_6Sn_6 and RFe_6Ge_6 systems, with *R* being alkali metals and rare earth metals, are predicted to exhibit strong anomalous transport, which calls for a systematic study.

Furthermore, a handful of distorted kagome systems have drawn researcher's attention recently, which also hold complex magnetic phase transitions and topological transport phenomena. We also aim to further investigate the ONE in transition-metal pnictides. There are numerous candidates for topological semimetals among the pnictides, such as $TaSb_2$, MoP, and WP_2. Although their electrical transport has been reported, their thermoelectric transport requires further investigation.

Finally, we plan to study additional topological insulators as magneto-thermoelectric materials and more doping effect of the current Bi–Sb system, and searching for new materials.

External Cooperation Partners

Sarah Watzman (University of Cincinnati); Toni Helm (Helmholtz-Zentrum Dresden-Rossendorf); and Joseph P. Heremans (The Ohio State University).

References

[1]* *Giant anomalous Nernst signal in the antiferromagnet $YbMnBi_2$, Y. Pan, C. Le, B. He, S. J. Watzman, M. Yao, J. Gooth, J. P. Heremans, Y. Sun and C. Felser, Nat Mater **21** (2022) 203–209, https://doi.org/10.1038/s41563-021-01149-2*

[2]* *Anomalous thermoelectric effects and quantum oscillations in the kagome metal CsV_3Sb_5, D. Chen, B. He, M. Yao, Y. Pan, H. Lin, W. Schnelle, Y. Sun, J. Gooth, L. Taillefer and C. Felser. Phys Rev B **105** (2022) L201109, https://doi.org/10.1103/PhysRevB.105.L201109*

[3]* *Ultrahigh transverse thermoelectric power factor in flexible Weyl semimetal WTe_2, Y. Pan, B. He, T. Helm, D. Chen, W. Schnelle and C. Felser, Nat Commun **13** (2022) 3909, https://doi.org/10.1038/s41467-022-31372-7*

[4] *Multiband synergy towards high thermoelectric performance in topological semimetal $TaAs_2$, H. Hu, X. Feng, V. Hasse, H. Wang, Y. Pan, B. He and C. Felser, in preparation.*

[5]* *Magneto-engineering towards high thermoelectric performance in topological insulator $Bi_{88}Sb_{12}$, Y. Pan, B. He, X. Feng, F. Li, D. Chen U. Burkhardt and C. Felser., Nat Mater accepted. (2024). Preprint at: https://doi.org/10.21203/rs.3.rs-3066848/v1*

[6]* *Catalogue of Phonon Instabilities in Symmetry Group 191 Kagome MT_6Z_6 Materials, X. Feng, Y. Jiang, H. Hu, D. Calugalu, N. Regnault,M. G. Vergniory, C. Felser, S. Blanco-Canosa, and B. Andrei Bernevig, in preparation.*
*See also **TQC_03_Feng***

[7]* *Giant anomalous Hall effect and band folding in a Kagome metal with mixed dimensionality, E. Cheng, K. Wang, S. Nie, T. Ying, Z. Li, Y. Li, Y. Xu, H. Chen, R. Koban, H. Borrmann, W. Schnelle, V. Hasse, M. Wang, Y. Chen, Z. Liu, and C. Felser, ArXiv (2024), https://arxiv.org/abs/2405.16831*

[8] *Record zT in Bi_xSb_{1-x} achieved by 1-D Landau level quantization, B. He, Y. Pan, X. Feng, D. Chen, F. M. Serrano-Sanchez, M. Nawwar, H. Hu, U. Burkhardt, B. Goodge, J. P. Heremans, C. Felser, in preparation.*

[#] yu.pan@cpfs.mpg.de
[##] bin.he@cpfs.mpg.de